THE UNIVERSITY OF MICHIGAN

COLLEGE OF ENGINEERING

Department of Aerospace Engineering

High Altitude Engineering Laboratory

Technical Report

Radiative Transfer in the Mesosphere

William Kuhn

ORA Project 05863

under contract with:

NATIONAL AERONAUTICS AND SPACE ADMINISTRATION

CONTRACT NO. NASr-54(03)

WASHINGTON, D. C.

administered through

OFFICE OF RESEARCH ADMINISTRATION ANN ARBOR

December 1968

TABLE OF CONTENTS

ABSTRACT

The determination of radiative temperature changes for molecular gases under non LTE conditions is discussed, with special emphasis on the microscopic formulation of the transfer equation. The radiative transfer and statistical equilibrium equations are combined to yield an explicit expression for the radiative temperature change. This method is applied to the 15μm and 4.3μm CO_2 transitions.

Mesosphere and lower thermosphere heating and cooling rates are calculated for the 15μm CO_2, 9.6μm O_3, and the 80μm H_2O bands and the spectral region from 1350 to 7550 Å, representing absorption of solar energy by O_3 and O_2. Maximum heating is found at the stratopause (5 deg per day) and mesopause (18 deg per day) over the summer pole while radiative cooling predominates in similar regions (-7 and -10 to -25 deg. per day respectively) over the winter pole. In the lower thermosphere, the radiative temperature change is strongly dependent on the collisional relaxation time.

The importance of the 4.3μm transition to radiative heating is demonstrated. Heating from this band is at least 1 deg per day in the vicinity of 70 km; however, a resonance exchange of the ν_3 mode of CO_2 with N_2 may occur which could lead to a heating at least three times larger than the non resonant heating. These calculations indicate the importance of collisional and radiative rates to upper mesosphere and lower thermosphere radiative heating and cooling.

1. Introduction

Within the last few years, our understanding of the radiational contribution to the thermal structure of the mesosphere has increased appreciably. Some of the techniques applicable to a radiation study of the lower atmosphere apply to this region also, although new problems, which we shall discuss below, cause the problem to be more formidable.

In the lower atmosphere we rely on the macroscopic parameters such as temperature to describe the system, while for the upper atmosphere we must inquire into the molecular nature of the gas. The approach used by astrophysicists to radiation transfer by atomic transitions, which we will show can be used for vibrational-rotational transitions, involves the statistical equilibrium equation as well as the radiative transfer equation. These two equations are coupled by the radiation field, and a solution to the radiative problem requires a knowledge of the molecular parameters such as radiative and collisional transition rates. A better understanding of these parameters is required before the upper mesosphere and lower thermosphere radiation problem will be adequately solved.

Other problems exist but they are more of a technical nature; increasing amounts of geophysical data are giving us a more accurate picture of the mesosphere, and the capability of present day computers allows us, in most cases, to adequately solve the transfer equation if we know the molecular parameters.

In this paper, I shall briefly review the microscopic formulation of the transfer equation. The major difficulties which one encounters in solving the transfer equation for mesospheric conditions will be noted and the latest results for radiative flux divergences in the mesosphere will be discussed.

2. Theory

The rate at which radiation is attempting to modify the temperature distribution is given by the formula

$$\frac{\partial T}{\partial t} = -\frac{1}{\rho c_p}\frac{\partial F}{\partial z} \tag{1}$$

where $\partial T/\partial t$ is the time rate of change of atmospheric temperature, ρ is the air density, c_p is the specific heat of air at constant pressure and $\partial F/\partial z$ is the vertical component of the flux divergence of radiation. If the flux divergence is positive there is a transformation of energy from the matter or thermal field to the radiation field and the atmosphere acts as a radiation source. If on the other hand, the flux divergence is negative, the rate of temperature change is positive and the atmosphere acts as a radiation sink. Often it is more convenient to express the time rate of change of temperature as

$$\frac{\partial T}{\partial t} = \frac{g}{c_p}\frac{\partial F}{\partial p} \tag{2}$$

where use has been made of the hydrostatic equation,

$$dp = -\rho g dz$$

where p is pressure, and g is the acceleration due to gravity.

The flux of radiation, $F(u_o)$, can be found from an integral form of the radiative transfer equation,

$$F(u_o) = \sum_i \pi\left[B_i(0)\,\tau_i(u_o) + \int_0^{u_o} S_i(u)\,\frac{d\tau_i(u_o-u)}{du}\,du\right]\delta_i - \tag{3}$$

$$-\sum_i\left[B_i(\infty)\,d\cdot\sec\chi\cdot\tau(u_\infty-u_o) + \pi\int_u^{u_o} S_i(u)\,\frac{d\tau_i(u-u_o)}{du}\,du\right]\delta_i$$

where $B_i(0)$, $B_i(\infty)$ = Planck function at the surface of the earth, and top of atmosphere, respectively.

τ_i = the flux transmissivity for the wave number interval of width δ_i

S = source function

d = dilution factor for boundary flux (solar radiation) incident on the top of the atmosphere.

χ = zenith angle of the sun

u = mass path of absorbing gas measured positive from the surface of the earth.

If the mixing ratio of the particular gas which is absorbing and emitting radiation and the temperature and pressure are known functions of height, then the transmission can be determined. A knowledge of the source functions will then allow one to determine directly from (3) the net flux. For the lower atmosphere, say up to approximately 70 km, the source function depends on one atmospheric parameter, the kinetic temperature, which is uniquely determined for every height in the atmosphere. The expression for the source function is then just the familiar Planck function. Now if the source function cannot be approximated by the Planck function, the source function is not only dependent on the local kinetic temperature, but it depends also on the radiation field in the particular region where the source function is to be determined. This radiation field in turn depends on the overall thermal structure of the atmosphere, and a second expression, the statistical equilibrium equation, which relates the source function to the radiation field, is required. With these two independent expressions the flux and the flux divergence can then be calculated. The analytical formulation of the problem is discussed below.

The macroscopic form of the transfer equation for a molecular transition can be given as

$$\mu \frac{dI_\omega}{d\tau_\omega} = I_\omega - S_\omega \qquad (4)$$

where μ is the cosine of the zenith angle made by the normal to the atmosphere and the specific intensity I_ω, τ_ω is the optical depth, and S_ω is the source function. The above equation could also be derived (see, e.g. Thomas 1965) in terms of the molecular parameters for which case,

$$d\tau_\omega = -hc\omega n_\ell B_{\ell u}(1 - n_u g_\ell / n_\ell g_u)\, dz \qquad (5)$$

and

$$S_\omega = 2hc^2\omega^3 \left(n_\ell g_u / n_u g_\ell - \frac{\Psi}{\Phi}\right)^{-1} \frac{j}{\Phi} \qquad (6)$$

where

h = Planck's constant

c = speed of light

ω = wave number for the particular transition

n_u, n_ℓ = number density for molecules in upper and lower energy state respectively, with corresponding statistical weights g_u, g_ℓ.

$B_{\ell u}$ = Einstein absorption coefficient

Ψ, Φ, j = profile functions for stimulated emission, absorption, and spontaneous emission respectively.

This equation represents the transfer of radiation for a particular molecular transition, i.e., either electronic, vibrational, or rotational.

If the gas is so dense that collisions are primarily responsible for populating the energy levels of the transition in question, the familiar Boltzmann distribution can be used in (6), the profile parameters will be identical, and the source function

reduces to the Planck function. If, however, collisions are so infrequent that radiative transitions influence the population densities, then the Boltzmann distribution is no longer applicable and the source function depends on the incident radiation field. In this case a second expression relating the population densities to the radiation field is required. Such an expression is the statistical equilibrium equation.

In statistical equilibrium we assume that the population densities of the levels in question do not vary with time. Thus any processes which tend to change population densities of the energy levels occur at a much slower rate than the rate at which collisions and/or radiative transitions tend to maintain that distribution. This assumption is true for processes which occur in planetary atmospheres and we can express the condition of statistical equilibrium analytically as (Jefferies, 1960)

$$\frac{n_u}{n_l} = \frac{\sum_{k \neq l} P_{lk} q_{ku,l}}{\sum_{k \neq u} P_{uk} q_{kl,u}} \qquad (7)$$

where $q_{ab,c}$ is the probability for all transitions from level a to b not involving c, except when a = b, for which case $q_{aa,c} = 1$; P_{ab} refers to the rate of transitions from level a to b and includes both radiative and collisional transitions; thus we have a second independent relationship relating the population densities to the radiation field. This equation can then be combined with (6), and the source functions and radiative temperature changes determined simultaneously (Kuhn and London, 1968).

For mesospheric thermal radiation calculations, the infrared or vibration-rotation transitions are primarily responsible for transferring the planetary radiation. As an example, we consider

the 15μm CO_2 band (see Fig. 1) and some of the additional energy levels which could influence the radiative temperature change (hereafter designated as rtc) for this 15μm transition. Eqn. (7) then has the form,

Fig. 1

$$\frac{n_2}{n_1} = \frac{P_{12} + P_{13} q_{32,1} + P_{14} q_{42,1}}{P_{21} + P_{23} q_{31,2} + P_{24} q_{41,2}} \qquad (8)$$

where P and q are easily expressed in terms of the spontaneous ($A_{u\ell}$) and stimulated ($\bar{I}_{u\ell} B_{u\ell}$) emission, absorption ($\bar{I}_{\ell u} B_{\ell u}$), and collisional ($C_{u\ell}$, $C_{\ell u}$) rates, where, e.g.,

$$P_{21} = C_{21} + A_{21} + \bar{I}_{21} B_{21}$$

$$q_{32,1} = [A_{32} + C_{32} + \bar{I}_{32} B_{32} + C_{42}(C_{34} + \bar{I}_{34} B_{34}] / [A_{32} + C_{32} + \bar{I}_{32} B_{32} + C_{42}(C_{34} + \bar{I}_{34} B_{34}) + (C_{34} + \bar{I}_{34} B_{34})(C_{41} + A_{41} + \bar{I}_{41} B_{41})]$$

Neglecting stimulated emissions, which is justified for infrared transitions, (see e.g. Kuhn, 1968) and with values for collisional and radiative rates as given in Table 1, we find that the levels

Table 1. Spontaneous transition rates ($A_{u\ell}$), and collisional de-excitation rates ($C_{u\ell}$) for the transitions indicated in Figure 1. (Kuhn, 1968)

Transition	$A_{u\ell}(sec^{-1})$	$C_{u\ell}(sec^{-1})$ NTP
2-1	1.2	1.0×10^5
3-1		3.5×10^1
3-2	1.1×10^1	9.6×10^4
4-1	4.2×10^2	1.4×10^5
4-2	-	9.3×10^2
4-3	4.5×10^{-1}	5.7×10^4

001 and 100 make a negligible contribution to the population densities of 000 and 01^10 so that (8) may be approximated as,

$$\frac{n_2}{n_1} \sim \frac{\bar{I}_{12} B_{12} + C_{12}}{\bar{I}_{12} B_{21} + A_{21} + C_{21}} \qquad (9)$$

It should be noted that the rotational states have not been arbitrarily excluded from this calculation. It is only because the rotational states are still populated by a Boltzmann distribution at mesospheric levels that allows us to define a mean or effective radiative lifetime for the vibrational transition. Consider, e.g., the statistical equilibrium equation for a single vibration-rotational state J (Fig. 2)

$$\sum_\ell n(J_\ell)\, P(J_\ell, J) + \sum_u n(J_u)\, P(J_u, J) = \sum_\ell n(J)\, P(J, J_\ell) + \sum_u n(J)\, P(J, J_u) \qquad (10)$$

where V =1 and V = 2 refer to the vibrational states and J_l and J_u their corresponding rotational states.

Fig. 2

The first and third terms of (10) represent all transitions involving J between the two vibrational levels while the second and last terms represent all rotational transitions within the v = 2 level. Since the energy differences for rotational transitions are much smaller than for vibrational transitions, the influence of long range collisions will be more effective in establishing a Boltzmann distribution among the rotational states. Lambert (1962) has found that the average number of collisions required for a rotational de-excitation is less than 10, while for a vibrational transition the number of collisions is much higher (for the 15μm CO_2 band the number of collisions required is 10^5 to 10^6). Thus, rotational levels remain populated by a Boltzmann distribution to much higher elevations than do the vibrational levels, and consequently the principle of detailed balance (thermodynamic equilibrium) applies to the rotational transitions, and the second and last terms in (10) are identical. If we now sum the remaining two terms representing transitions between the two vibrational levels over all J_u states, we find for the ratio of the total number of molecules in the two vibrational levels,

(11)

$$\frac{n_2}{n_1} = \frac{\sum_u \sum_l \varphi_l [\bar{I} B(J_l, J_u) + C(J_l, J_u)]}{\sum_u \sum_l \varphi_u [\bar{I} B(J_u, J_l) + A(J_u, J_l) + C(J_u, J_l)]}$$

where

ϕ_ℓ (ϕ_u) = the ratio of the number density of molecules in the rotational states J_ℓ, (J_u) to the total number of molecules in the v = 1 (v = 2) vibrational level.

$\bar{I}$ = $1/4\pi \int\int I_\omega \kappa_\omega / \delta \, d\omega \, d\Omega$, the mean value of the radiation field, averaged over the vibration-rotation band and solid angle Ω . δ represents the total line strength for any particular line and κ_ω / δ is the profile parameter for absorption.

Since we have assumed that the rotational states are in thermodynamic equilibrium, the double summations over each term represent the mean radiative and collisional rates for a single vibration rotation band (see, e.g., Penner, 1959); thus we have

$$A_{21} = \sum_u \sum_\ell \phi_u \, A(J_u, J_\ell) \Big/ \sum_u \phi_u$$

$$B_{21} = \sum_u \sum_\ell \phi_u \, B(J_u, J_\ell) \Big/ \sum_u \phi_u$$

$$B_{12} = \sum_u \sum_\ell \phi_\ell \, B(J_\ell, J_u) \Big/ \sum_\ell \phi_\ell \qquad (12)$$

$$C_{12} = \sum_u \sum_\ell \phi_\ell \, C(J_\ell, J_u) \Big/ \sum_\ell \phi_\ell$$

$$C_{21} = \sum_u \sum_\ell \phi_u \, C(J_u, J_\ell) \Big/ \sum_u \phi_u$$

Substituting (12) into (11), we find that this latter equation is then formally identical to (9).

If we make use of the well-known relations (see, e.g., Milne, 1930)

$$\begin{aligned} A_{21} &= 2hc^2\omega^3 B_{21} \\ B_{21} &= (g_1/g_2) B_{12} \\ C_{21} &= (g_1/g_2) C_{12} \exp(hc\omega/kT) \\ B &= 2hc^2\omega^3 (\exp(hc\omega/kT) - 1)^{-1} \end{aligned} \tag{13}$$

we find for the source function

$$S_{12} = \frac{\bar{I}_{12} + \epsilon B}{1 + \epsilon} \tag{14}$$

where $\epsilon = C_{21}/A_{21}(1 - \exp(-hc\omega/kT))$. For infrared bands at terrestrial temperatures (e.g., for the 15μm CO_2 band at T = 250 K) the quantity $(1 - \exp(-hc\omega/kT)) \sim 0.98$ which gives $\epsilon \sim C_{21}/A_{21}$.

The source function for the two level molecule can be expressed in terms of the rate of temperature change in the following way: Assume the vibration-rotation lines do not overlap. Then $\int_{\text{band}} \kappa_\omega d\omega = \mathcal{S}_b$, the band strength, and (14) can be written,

$$S_\omega = \left[\frac{\int\int I_\omega \kappa_\omega \, d\omega \, d\Omega}{4\pi \mathcal{S}_b} + \epsilon B \right] / (1 + \epsilon) \tag{15}$$

The radiative transfer equation for the net integrated flux is,

$$-\frac{\partial F}{\partial z} = \rho_a g \frac{\partial F}{\partial p} = \iint K_\omega \rho_g I_\omega \, d\omega \, d\Omega - \iint K_\omega \rho_g S_\omega \, d\omega \, d\Omega \quad (16)$$

and substitution of (16) into (15) with S assumed isotropic and wavenumber independe ; over the band gives,

$$S(p) = B(p) + \frac{g}{4\pi \beta_b w(p) \cdot \epsilon(p)} \frac{\partial F[S(p)]}{\partial p} \quad (17)$$

where w is the mixing ratio of gas. The rate of temperature change for the band is then given by (2). We can now write an equation of the form of (17) for each atmospheric layer. Each equation is coupled to the equations of the remaining layers through the source functions. Once the transmission functions are evaluated, our problem consists in solving the system of simultaneous equations, which are equal in number to the number of atmospheric layers. Of course, if the source function can be expressed by the Planck function, then the radiative heating or cooling can be calculated directly from (2) and (3).

The result for this "two level" calculation is shown in Fig. 3. The source function for the 15μm band of CO_2 is given by the Planck function up to the height of the mesopause. Above this elevation the source function, in general, decreases while the Planck function, which follows the temperature distribution, increases. One would expect that a deviation between the Planck function and the source function would first occur when the radiative and collisional rates are comparable, i.e., $\epsilon \sim 1$. For the 15μm transition this does indeed occur near the mesopause height.

Fig. 3

3. Transmission functions

The transmission functions which are required in order to solve the transfer equation may be evaluated by utilizing either

the actual positions and strengths of lines within the band or by an appropriate band model. Since the former method is very time consuming even with present computer facilities, we have used the quasi-random band model (Stull et al, 1964). We assumed a Curtis-Godson approximation, and the appropriate profile function, Voigt or Doppler, was determined (Kuhn, 1966). A sample flux transmissivity function for CO_2 is shown in Fig. 4.

Fig. 4

This calculation, made for 5 cm^{-1} intervals, reproduces the general contour of the band. The uppermost curve shows the transmission for a 10 km layer centered at 90 km; practically all the transmission takes place in the spectral region 620 to 720 cm^{-1}, with the Q branch being of primary importance. Similar calculations were made for the 9.6μm O_3 and 80μm H_2O bands, with spectral line data from Kaplan, Migeotte, and Neven (1956), and Walshaw and Goody (1954) for the 9.6μm band, and from Benedict (unpublished) and Yamamoto and Onishi (1951) for the 80μm band.

It is important to note that non-LTE calculations require only an average transmission for the band since the wave number dependence of the source function is neglected. When the source function is approximated by the Planck function then the transfer equation can be solved for an arbitrary wave number increment in the band and an equation of the form of (3) would be solved for each wave number increment.

Approximations which were made in computing the infrared transmission functions as well as uncertainties in the band parameters were tested to determine their influence on the rtc; these tests were carried out for the 15μm CO_2 band although, in

most cases they will also give an estimate for the other bands as well (Kuhn, 1966):

i. Line broadening; throughout the lower mesosphere, both Lorentz and Doppler broadening influence the spectral distributions of radiation and the Voigt profile must be used. Above approximately 70 km Lorentz broadening is negligible, and the Doppler profile is adequate.

ii. Uncertainties in line half-width; rtc was computed for surface collision half widths of 0.064 and .1 cm^{-1}. The larger half width gives a rtc approximately 15% higher near the stratopause than the 0.064 cm^{-1} half width. At 72 km the difference is negligible. The variation of Doppler half width with wave number over the band is also negligible. A Doppler half width computed for a 200 K temperature gives a rtc which differs from that for a 300 K temperature by approximately 10% in the upper mesosphere. Since the temperature variation in a mesospheric region contributing to a rtc is much less than 100 K, the variation of Doppler line half width with temperature is also negligible.

iii. Weak lines; if the lines which are five orders of magnitude weaker than the strongest lines in the band are neglected, the resulting error in the rtc is less than 3% in the mesosphere.

iv. Temperature dependence of the line strengths; a 300 K line strength gives a rtc approximately 45% larger than a 200 K line strength, while a 250 K line strength gives a rtc 85% as large as a 300 K line strength. A 250 K line strength gives results which are within 10%

of those for a variable temperature line strength between 30 and 70 km. From 70 km to the lower thermosphere, a 200 K line strength gives similar errors.

4. Mesospheric radiative temperature changes

An example of the rtc for the 15μm CO_2 band is given in Fig. 5 (Kuhn and London, 1968). The pattern of radiative cooling is similar to the temperature distribution in the upper stratosphere and mesosphere. At the mesopause, in the region of the

Fig. 5

temperature minimum, there is a convergence of radiation. Above the mesopause, cooling again predominates, reaching a maximum in the lower thermosphere; the Planck function, which increases with elevation, and the decreasing collisional rate produce this local maximum in the source function (see Fig. 3). As demonstrated in Fig. 5, the cooling in the lower thermosphere is strongly dependent on the collisional rate.

Our results are quite similar to those of Plass (1956), although this may be somewhat fortuitous in view of the different temperature profiles used as well as the differences in the transmission functions. In the lower mesosphere our values are approximately 30% larger than those of Plass although he indicates that his values may be quite inaccurate at these mesospheric elevations. Nevertheless, agreement is quite good if one contrasts the methods used in each case. Calculations recently completed by Drayson (1967) are also shown. His calculations represent a direct integration with respect to wave number across the band. He also permitted the source function to vary linearly with pressure within each horizontal atmospheric layer, whereas we considered homogeneous "slabs". His values are approximately

1 - 2 deg per day larger than ours, and this discrepancy has not been completely resolved.

A net rtc including the effects of both solar and planetary radiation is given in Fig. 6. The bands considered are the 15μm CO_2, the 9.6μm O_3, the 80μm H_2O, and the spectral region from 1350 to 7550 Å, representing absorption of solar energy by O_3 and O_2. The mixing ratios for CO_2 and H_2O are 4.56×10^{-4} and 10^{-6} respectively, and the O_3 profiles are from London (1968). The assumed temperature distributions are from Kantor and Cole (1965), Teweles (1963), and Maeda (1962).

Fig. 6

Maximum heating is, in general, found at the stratopause and mesopause over the summer pole while the maximum radiative cooling is found in similar regions over the winter pole. The maximum heating results primarily from the high absorption by O_3 at summer latitudes and infrared convergence at the cold summer polar mesopause. The cooling at the winter pole results from infrared emission and the absence of solar heating. In the lower thermosphere, the rtc is strongly dependent on the collisional relaxation time. This region acts primarily as a radiation sink if the surface relaxation time is 2×10^{-5} sec, but a time of 2×10^{-6} sec produces a radiation source (Fig. 7).

Fig. 7

CO_2 is the primary contributor to radiative cooling in the mesosphere. This cooling is approximately 6 deg per day at the stratopause, decreasing to zero at 75 km. There is a heating of a few deg per day in the mesopause. In the lower thermosphere the values for radiative cooling are subject to speculation because of uncertainty in the collisional rate (compare Fig. 6 and 7).

The 9.6μm O_3 band contributes to radiative cooling in the mesosphere, this cooling rate being largest at the stratopause (3 deg per day) and decreasing and becoming negligible in comparison to the CO_2 cooling at 70 km. Non LTE calculations are not required for this 9.6μm transition.

The 80μm H_2O band produces maximum radiative cooling of 1 deg per day near the equatorial stratopause. This cooling decreases with increasing latitude and elevation, becoming negligible at 65 km. Non LTE effects are negligible for this rotational band.

Absorption of solar radiation by O_3 produces a heating of approximately 14 deg per day during the summer near the stratopause. During the winter there is a uniform decrease in this heating rate from 13 deg per day at the equator to 4 deg per day at 60° latitude. Throughout most of the mesosphere, O_3 and O_2 produce a heating of 8-10 deg per day during the summer, and in winter the heating decreases from 7 deg per day at the equator to 2-4 deg per day at 60° latitude. At the mesopause, O_2 produces a heating during the summer of 14 deg per day; during the winter the heating decreases from 14 deg per day at the equator to 2 deg per day at 60° latitude.

The results, as shown in Fig. 6, are qualitatively similar to those of Murgatroyd and Goody (1958), although there are notable exceptions. In general, their cooling values are larger than ours. This is particularly so in the polar regions during the winter where they find two levels of maximum cooling; one at 65 km (15 deg per day) and the other at 90 km (17 deg per day). Our results show maxima of 6 deg and 12 deg per day (for $\lambda = 2 \times 10^{-5}$ sec) at 55 km and 90 km respectively. During the summer Murgatroyd and Goody find a region of low latitude cooling and upper and mid

latitude radiative heating while we find a general heating throughout the mesosphere during the summer. Even so, the general agreement of ıe results of Murgatroyd and Goody with those presented here is quite good, particularly in view of the many approximations made by them.

Fig. 8

The absorption bands considered above are, at present, thought to be the major contributors to the mesospheric rtc. However, few estimates have as yet been made for the contributions of the shorter wavelength bands of the CO_2 molecule. As an example, consider the 4.3 μm band (Fig. 8, (Kuhn, 1968)). The non LTE heating rate, due primarily to absorption of solar radiation is a maximum near 70 km with a value of approximately 1 deg per day which is comparable to the heating rate of the 15 μm CO_2 band. However, it has been suggested that a resonance exchange between the ν_3 mode of CO_2 and the v = 1 level of N_2 may occur (Taylor and Bitterman, 1967),

$$CO_2^*(\nu_3) + N_2 \longrightarrow CO_2 + N_2^* + 18\ cm^{-1}$$

with a corresponding relaxation time approximately two orders of magnitude smaller than the non resonant relaxation time of 7 microseconds. If, e.g., the relaxation time were 0.1 microseconds, the maximum heating from the ν_3 transition would peak at 82 km with a value of 3 deg per day. It does not at this time appear realistic to incorporate into a mesosphere radiation budget analysis the influences of minor bands of CO_2. While we can demonstrate the probable importance of these bands, nevertheless the collisional rates of these upperstate and overtone bands are not well known, and they will significantly influence the appropriate form of the statistical equilibrium equation.

Our knowledge of most collisional rates for transitions which may be of importance to mesospheric rtc is still quite uncertain. While some experimental and theoretical work has

been carried out in these areas, there has been little attempt to synthesize the results and incorporate those conditions such as temperature and composition which apply to the mesosphere. Until these collisional rates are known, upper mesosphere and lower thermosphere rtc will remain in some doubt.

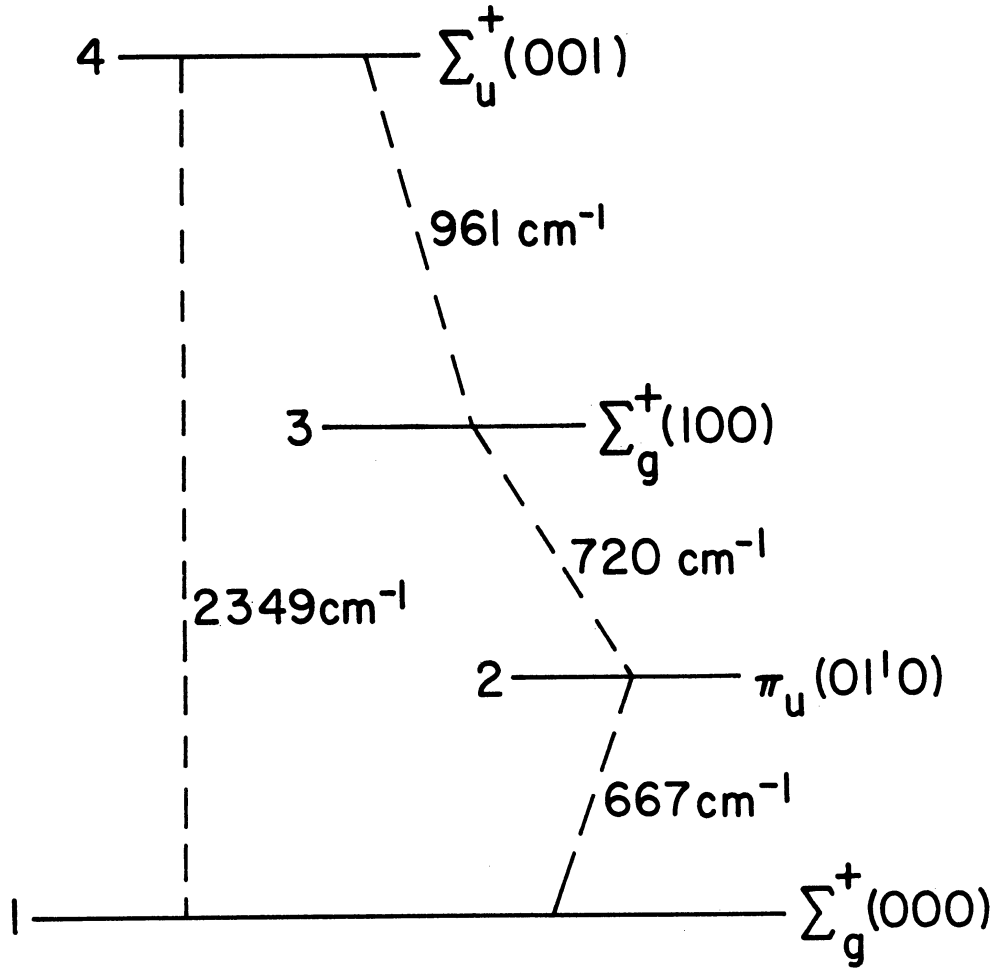

Fig. 1. Partial energy level diagram for the fundamental infrared transitions of the CO_2 molecule.

$$\sum_{\ell} n(J_\ell) P(J_\ell, J) + \sum_{u} n(J_u) P(J_u, J) = \sum_{\ell} n(J) P(J, J_\ell) + \sum_{u} n(J) P(J, J_u)$$

$$n(J_\ell)/n_1 = \varphi_\ell \quad , \quad n(J_u)/n_2 = \varphi_u$$

$$\frac{n_2}{n_1} = \frac{\sum_u \sum_\ell \varphi_\ell \left[\bar{I} B(J_\ell, J_u) + C(J_\ell, J_u)\right]}{\sum_u \sum_\ell \varphi_u \left[\bar{I} B(J_u, J_\ell) + A(J_u, J_\ell) + C(J_u, J_\ell)\right]}$$

$$A_{21} = \sum_u \sum_\ell \varphi_u A(J_u, J_\ell) / \sum_u \varphi_u$$

$$B_{21} = \sum_u \sum_\ell \varphi_u B(J_u, J_\ell) / \sum_u \varphi_u$$

$$B_{12} = \sum_u \sum_\ell \varphi_\ell B(J_\ell, J_u) / \sum_\ell \varphi_\ell$$

$$C_{12} = \sum_u \sum_\ell \varphi_\ell C(J_\ell, J_u) / \sum_\ell \varphi_\ell$$

$$C_{21} = \sum_u \sum_\ell \varphi_u C(J_u, J_\ell) / \sum_u \varphi_u$$

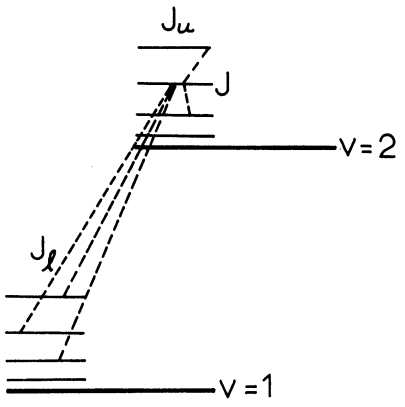

$$\frac{n_2}{n_1} = \frac{\bar{I} B_{12} + C_{12}}{\bar{I} B_{21} + A_{21} + C_{21}}$$

Fig. 2. Energy level diagram for a vibrational rotational band.

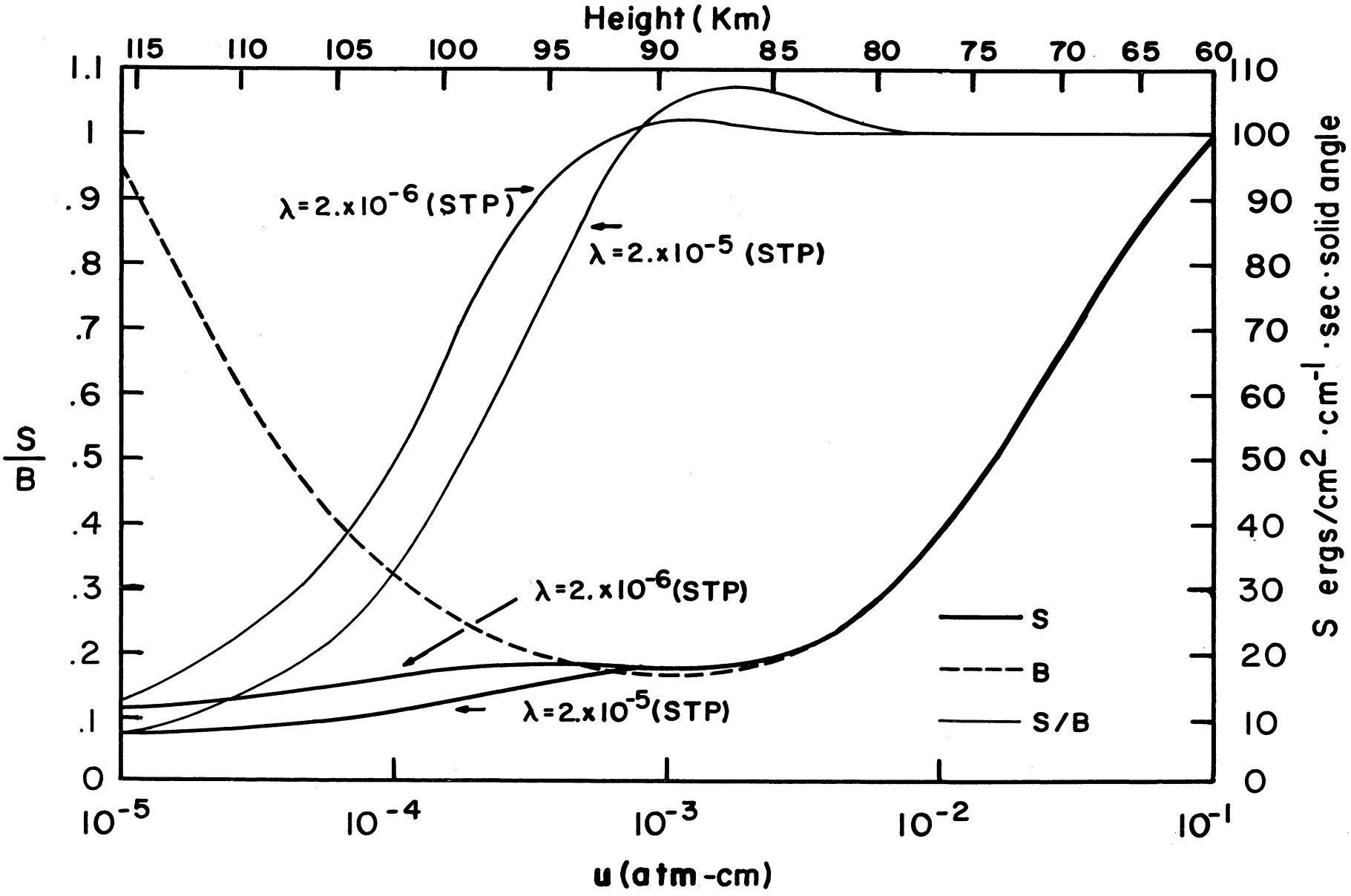
Height (Km)
115
110
105
100
95
90
85
80
75
70
65
60
1.1
1
.9
.8
.7
.6
.5
.4
.3
.2
.1
0
S/B
110
100
90
80
70
60
50
40
30
20
10
0
S ergs/cm² ·cm⁻¹ ·sec ·solid angle
λ=2.x10⁻⁶ (STP)
λ=2.x10⁻⁵ (STP)
λ=2.x10⁻⁶(STP)
λ=2.x10⁻⁵(STP)
S
B
S/B
10⁻⁵
10⁻⁴
10⁻³
10⁻²
10⁻¹
u (atm-cm)

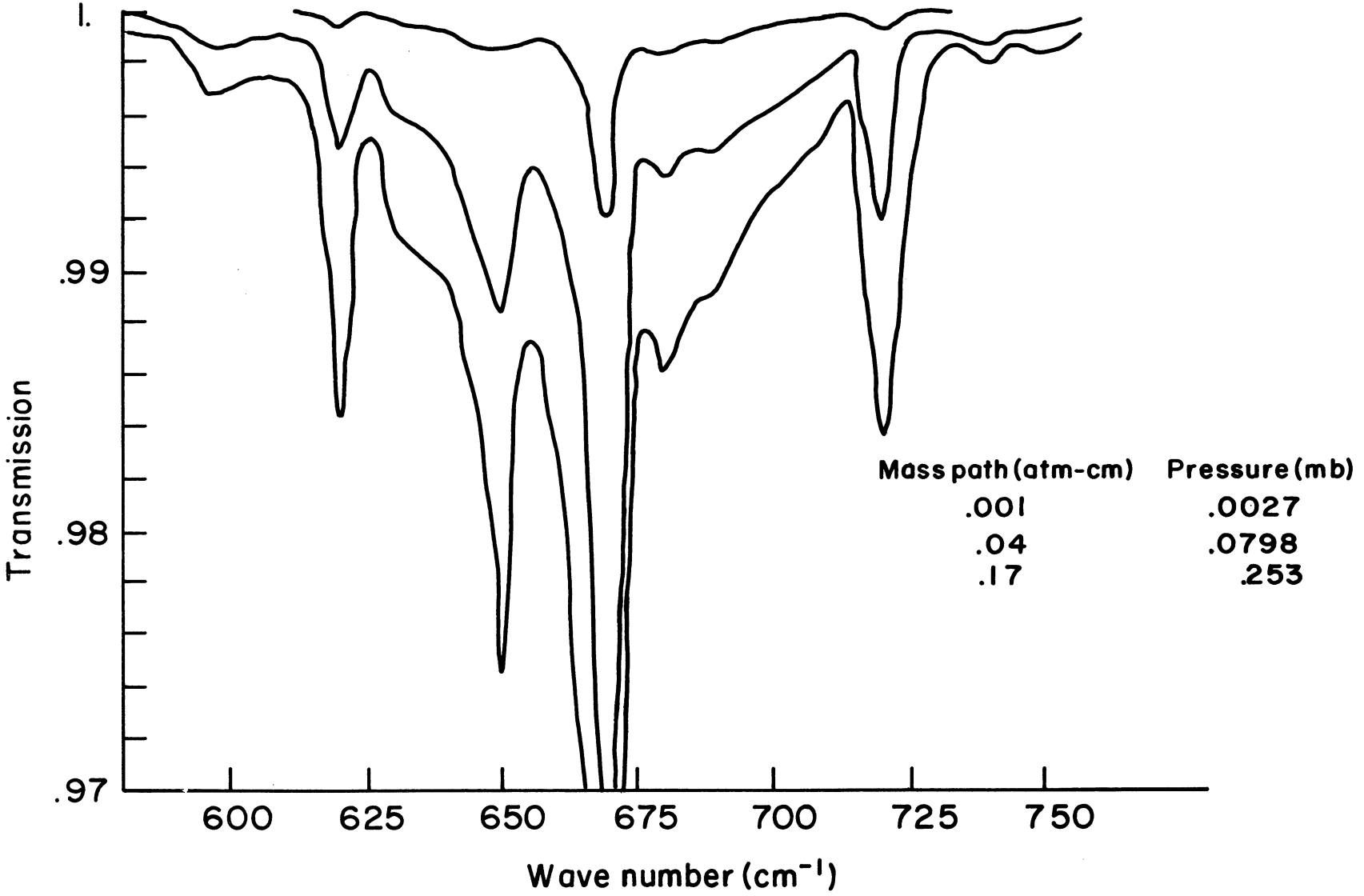

Fig. 4. Transmission profiles for the 15 μ m CO_2 band.

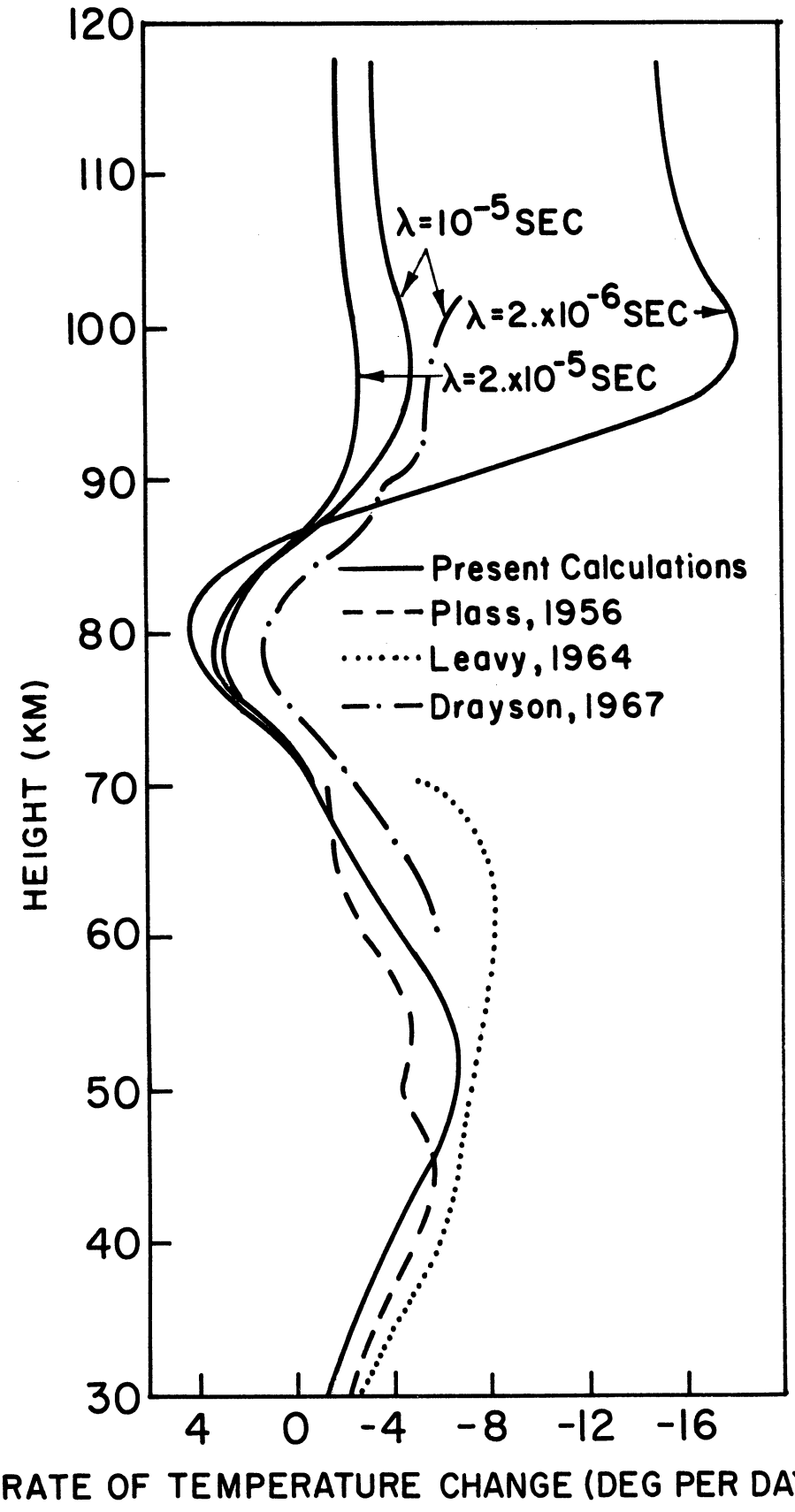

Fig. 5. rct for the 15 μm CO_2 band and comparisons. Temperature distribution for present calculations from U. S. Standard Atmosphere, 1962.

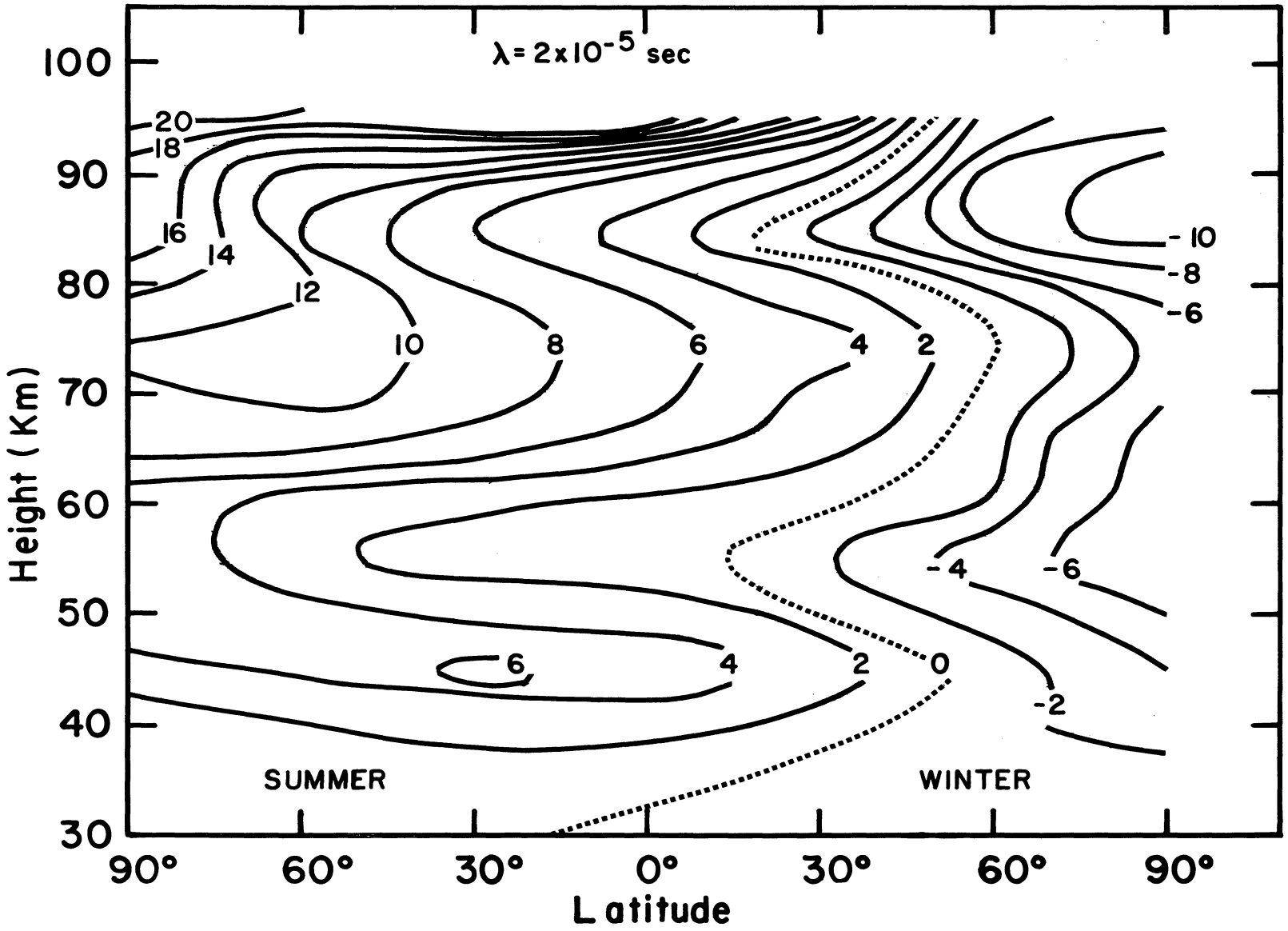

Fig. 6. Latitudinal distribution (for summer and winter) of net radiative temperature change. $\lambda = 2\text{x}10^{-5}$ sec for the 15 μm CO_2 transition.

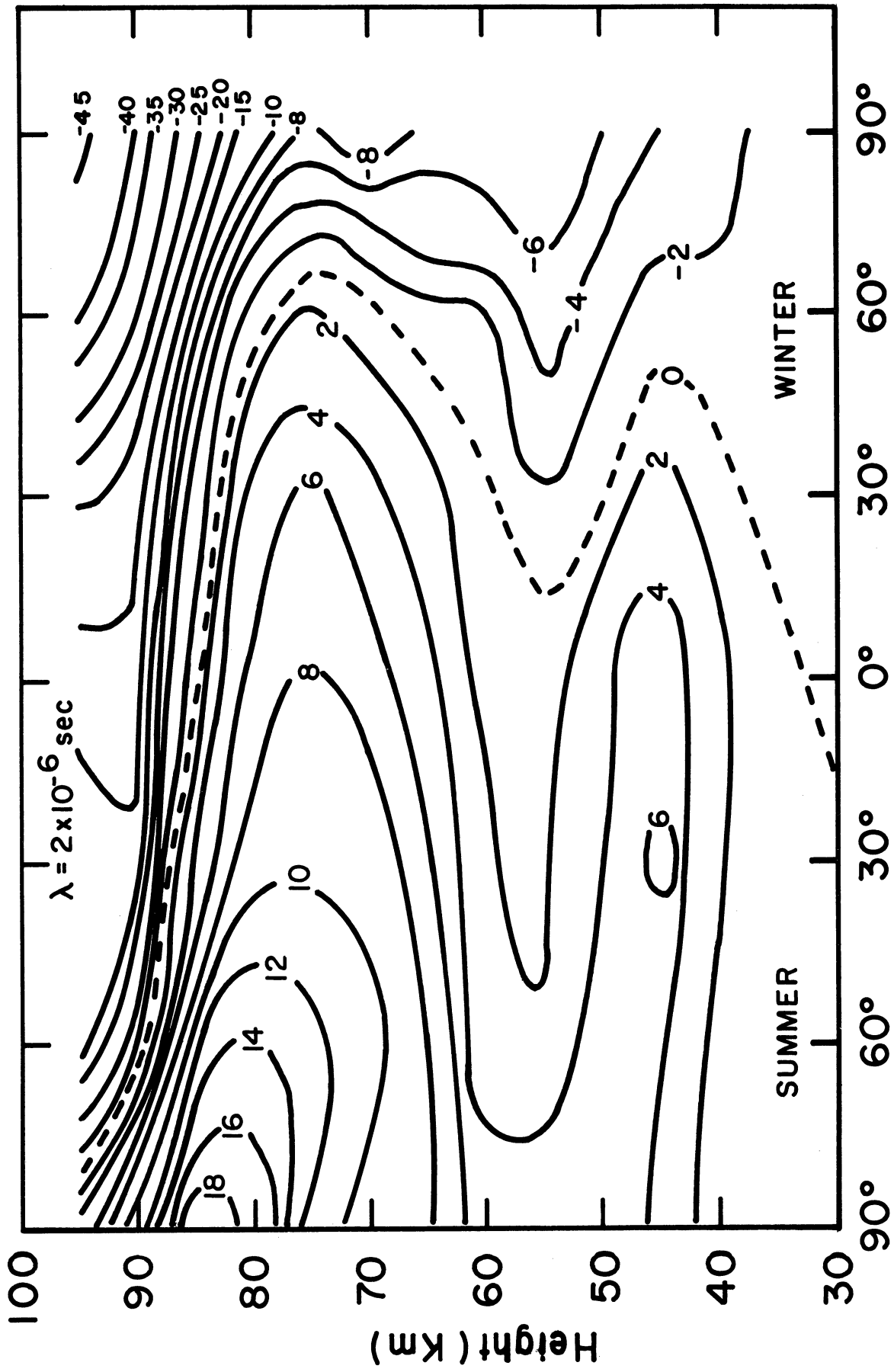

Fig. 7. Latitudinal distribution (for summer and winter) of net radiative temperature change. $\lambda = 2 \times 10^{-6}$ sec for the 15 μm CO_2 transition.

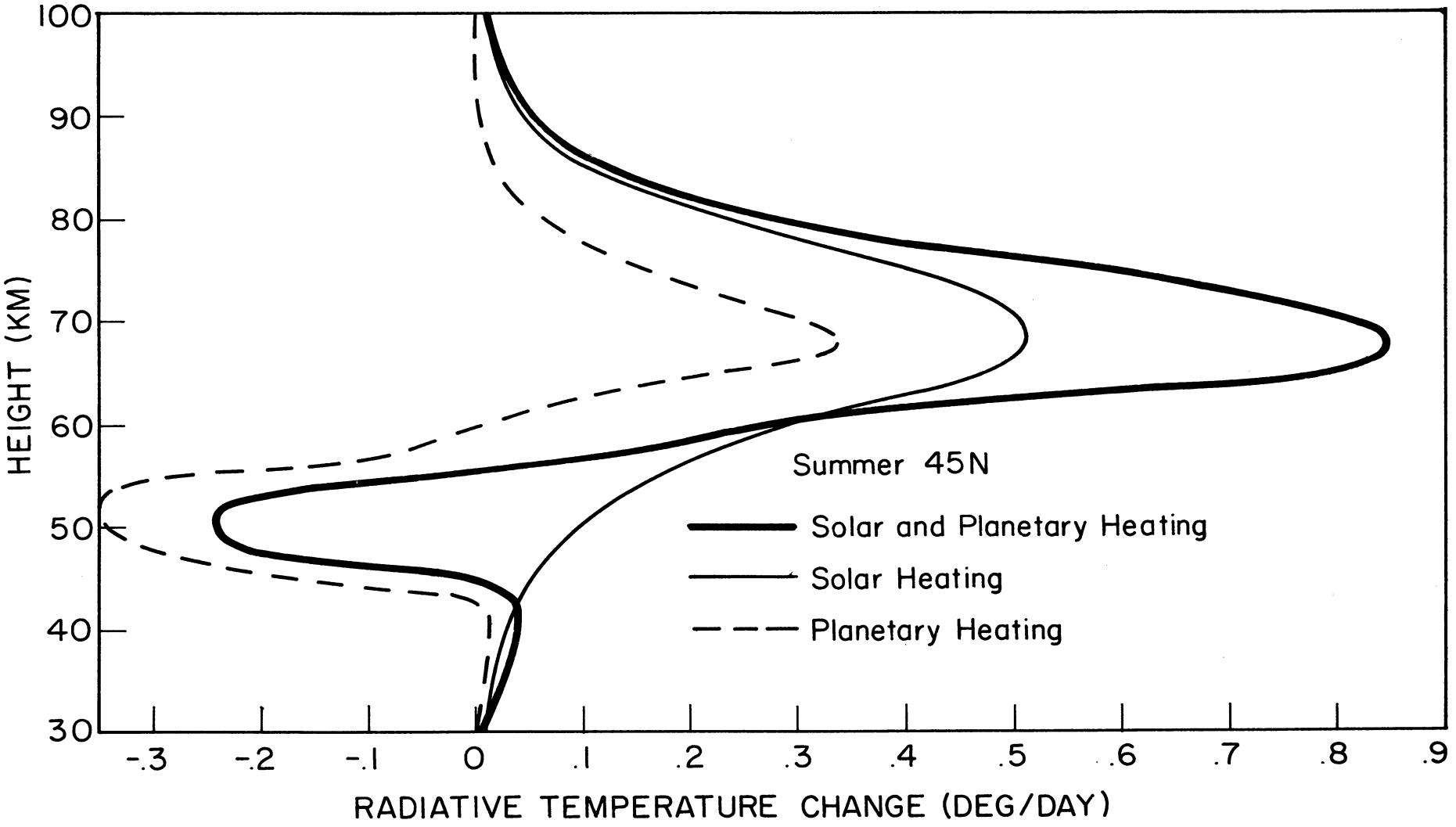

Fig. 8. rtc for the 4.3 μm CO_2 band with a non LTE formulation $\lambda = 7 \times 10^{-6}$ sec (STP).

REFERENCES

Benedict, W. S., unpublished data, 1965.

Drayson, S. R., College of Engr. Report No. 07584-1-T, Univ. of Michigan, Ann Arbor, 1967.

Jefferies, J. T., Astrophys. J., 132, 775, 1960.

Kantor, A. J., and A. E. Cole, J. Appl. Meteorol., 4, 1965.

Kaplan, L. D., et al., J. Chem. Phys., 24, 1956.

Kuhn, W. R., thesis, Univ. of Colorado, Boulder, 1966.

Kuhn, W. R., submitted for publication, J. Atmos. Sci., 1968.

Kuhn, W. R., and J. London, submitted for publication, J. Atmos. Sci., 1968.

Lambert, J. D., Atomic and Molecular Processes. ed. D. R. Bates, New York Academic Press, 1962.

London, J., unpublished data, 1968.

Maeda, K., NASA Technical Report, TR R-141, 1962.

Milne, E. A., Handbuch der Astrophysik, 3, ch. 2, 1930.

Murgatroyd, R. J., andR. M. Goody, Quart. J. Roy. Meteorol. Soc., 84, 1958.

Penner, S. S., Quantitative Molecular Spectroscopy and Gas Emissivities, Reading, Mass., Addison-Wesley, 1959.

Plass, G. N., Quart. J. Roy. Meteorol. Soc., 82, 1956.

Stull, V. R. et al., Report SSD-TDR-62-127, 3, Aeronutronic Div., Ford Motor Co., 1963.

Taylor, R. L., and S. Bitterman, Res. Rep. No. 282, Everett Res. Lab., Avco Corp., 1967.

Teweles, S., NASA Report No. SP-49, 1963.

Thomas, R. N., Some Aspects of Non-Equilibrium Thermodynamics in the Presence of a Radiation Field, Boulder, Colorado, Univ. of Colorado Press, 1965.

Walshaw, C. C., and R. M. Goody, R. Meteorol. Soc., 49, 1953.

Yamamoto, G., and G. Onishi, Sci. Reps. of the Tohoku Univ., Series 5, Geophysics, 3, 1951.